Chapter 3

BUILDING A NEURON MODEL OF A RAT SPINAL INTERNEURON

The previous chapter showed how simulation could be used to obtain a time series of the extracellular voltage, V_e, in a volume conductor model as a function of time for various electrode combinations. This chapter will discuss a computational model for a rat spinal interneuron. In the next chapters, the extracellular voltage from the volume conductor model will be applied to this neuron model to study the effect of epidural stimulation on neurons in the spinal cord. In particular, I will study if particular patterns of extracellular voltage from the epidural stimulation process can cause or facilitate the release of neurotransmitters from the tip of the axon.

The simulations of neuron dynamics used in this thesis are performed using NEURON version 7.3 (Michael L. Hines and Nicholas T. Carnevale, 1997). NEURON is a compartmental model neuron simulator. It simulates biological neurons by dividing each neuron into groups of compartments, called sections, which have similar membrane properties but may differ in diameter. The compartments in each section are referred to as segments and each may have a different diameter and 3D position. This thesis will not cover the background behind NEURON or compartmental modeling in detail. Readers unfamiliar with this material are encouraged to read (Michael L. Hines and Nicholas T. Carnevale, 1997). I will only cover the details necessary to reproduce the results reported in this thesis using the NEURON simulator.

Section 3.1 covers the neuron electrical properties which are used in the simulations. These properties are based on (Ostroumov, 2007). The model includes

sodium channels (INa), potassium fast channels (IK_A), and potassium delayed rectifier channels (IK_{dr}). In particular, the dendrites include sodium channels and potassium delayed rectifier channels, which means that the model described in this chapter includes active dendrites (dendrites with a non-linear response) rather than the passive dendrite model used in (Capogrosso et al., 2013). This section also discusses how the ion channels are modeled.

Section 3.2 covers the construction of a simple neuron model with 5 dendrites (with proximal and distal sections), a soma, and an axon (with axon hillock (AH), initial segment (IS), and axon proper sections). A simple constructed neuron model based on parameters from (Thurbon et al., 1998) and (Ostroumov, 2007) was chosen because of the difficulties in obtaining accurate 3D models of rat spinal interneurons and the increased computational demands of a complex model. It is hoped that results from this study will inspire further studies with more realistic neuron models.

Section 3.3 discusses models of neurotransmitter release from the axon tip due to neuron membrane activity (Section 3.3.2) and a synapse model (Section 3.3.1). In this thesis, a synapse is artificially triggered at specific times but would normally be triggered by neurotransmitters released by another neuron.

The simple neuron model is characterized in Section 3.4 so that it can be compared with neuron models and experimental data in other papers. Section 3.4.1 describes how the resting potential of the neuron was found. Section 3.4.2 describes the results of injecting 0.1 ms square current pulses into the neuron at each segment of the neuron. Section 3.4.3 finds the synapse weight thresholds for synapses placed in the interval from the soma to the distal tip of a dendrite. Sub-threshold synapse weights based on these thresholds are used in combination with sub-threshold stimulation to study facilitation in Chapter 5.

3.1 Model neuron properties

The membrane of a neuron cell is composed of a bilayer of lipid molecules which acts as an insulator. Various proteins are embedded in the lipid layers. Some of these proteins form ion channels which allow electrically charged ions to pass through the membrane. Many of these ion channels selectively allow only certain ions through in response to factors such as: membrane voltage, interactions with molecules outside or inside the cell, or the internal state of the ion channel. Other proteins in the membrane form ion pumps which push specific ions against the diffusion gradient to maintain the resting state of the neuron. The NEURON simulator models the ion pumps as a generalized leakage current across the membrane resistance (R_m) and a passive reversal potential (e_{pas}). Figure 3.1 shows the circuit representation of NEURON's model of a single compartment (segment) of a neuron.

The following properties of the neuron membrane were the same for all neuron sections used in the simulations and were taken from (Ostroumov, 2007):

- $e_{pas} = -70\,\mathrm{mV}$ (the reversal potential of the uniformly distributed leakage current)
- $e_{na} = 50.0\,\mathrm{mV}$ (the reversal potential of Na+ ions)
- $e_k = -77.0\,\mathrm{mV}$ (the reversal potential of K+ ions)
- $C_m = 2.4\,\mu\mathrm{F\,cm^{-2}}$ (the specific membrane capacitance)
- $R_m = 5300\,\Omega\,\mathrm{cm}^2$ (the membrane resistance)
- $R_a = 87\,\Omega\,\mathrm{cm}$ (the axial resistance)
- $R_{xraxial} = 1 \times 10^9\,\mathrm{M\Omega\,cm^{-1}}$ (the resistance of the extracellular medium along the axial direction, value is the NEURON default)

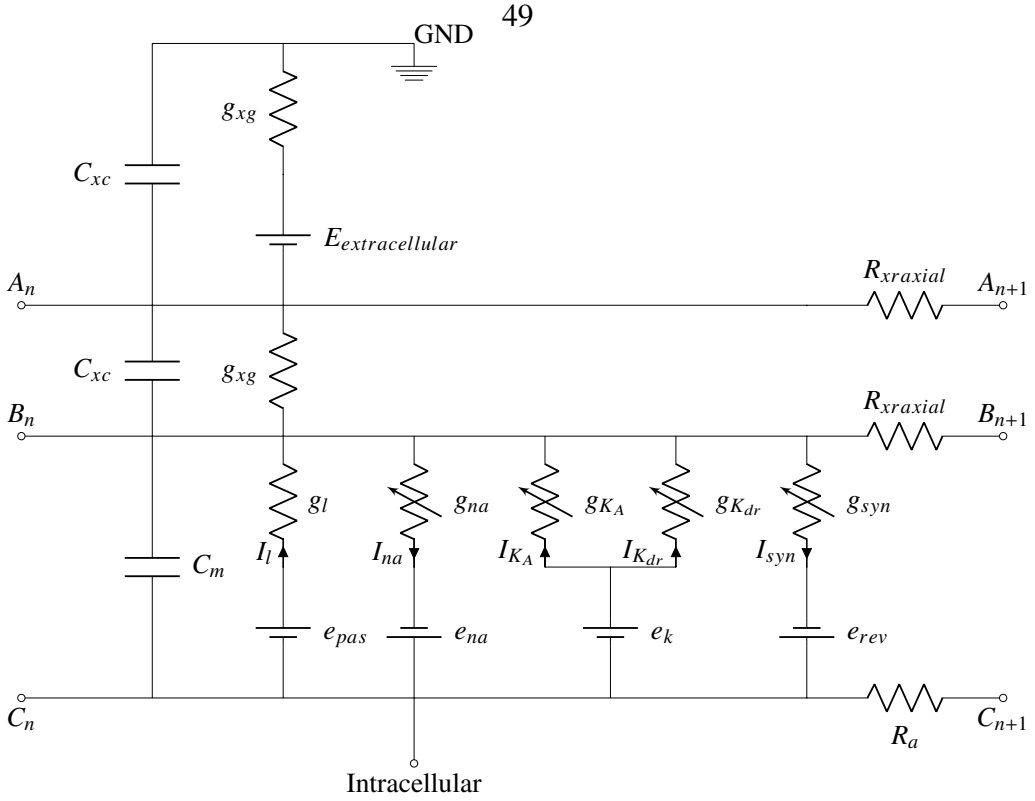

Figure 3.1: Neuron compartment circuit model for arbitrary compartment n including all modeled ion channels, a synapse, and extracellular voltage ($E_{extracellular}$). Points (A_n,B_n,C_n) connect to the corresponding points on the right hand side of compartment $n-1$. Starting from the bottom and going left to right,the components in the circuit are: the passive properties of the compartment which are modeled by the following components in the bottom left: the membrane capacitance (C_m), the membrane leakage conductance (g_l), and the reversal potential of the leakage current (e_{pas}). To the right of that is the sodium channel with variable conductance g_{na} (given by Eq. (3.1)) and e_{na} which is the reversal potential of Na^+ ions. To the right of that is the fast potassium channel with variable conductance g_{K_A} (given by Eq. (3.2)) and e_k which is the reversal potential of K^+ ions. The potassium delayed rectifier conductance ($g_{K_{dr}}$) is also connected to e_k and is given by Eq. (3.3). The synapse channel (only present if the compartment has a synapse attached) consists of the variable synaptic conductance g_{syn} (given by Eq. (3.5)) and the reversal potential of the synapse (e_{rev}). The axial resistance inside the neuron is modeled by resistance R_a. The upper portion of the circuit is the extracellular voltage mechanism of NEURON and is described in more detail in the NEURON documentation. $R_{xraxial}$ is the resistance of the extracellular medium along the axial direction. g_{xg} is the conductance of the extracellular medium between the extracellular potential and the membrane surface. C_{xc} is the capacitance of the extracellular medium (by default $C_{xc} = 0$ indicating an open circuit). $e_{extracellular}$ is the extracellular voltage which is obtained from the volume conductor models. Points (A_{n+1},B_{n+1},C_{n+1}) connect to the corresponding points in the next compartment ($n+1$).

- $g_{xg} = 1 \times 10^9\,\mathrm{S\,cm^{-2}}$ (the conductance of the extracellular medium between the extracellular potential and the membrane surface, value is the NEURON default)

- $C_{xc} = 0\,\mu\mathrm{F\,cm^{-2}}$ (the capacitance of the extracellular medium, value is the NEURON default)

The active ion channels (sodium channel, potassium fact channel, and potassium delayed rectifier channel) were taken from (Ostroumov, 2007). The maximum conductances of each channel in each section type are summarized in Table 3.1. The conductance of the sodium channel is given by:

$$g_{na} = g_{na,max} m_{ina}^3 h_{ina} \tag{3.1}$$

where $g_{na,max}$ is the maximum conductance of the channel given in Table 3.1, m_{ina} is the state variable of activation, and h_{ina} is the state variable of inactivation. The conductance of the potassium fast channel is given by:

$$g_{k_A} = g_{K_A,max} m_{ika}^4 h_{ika} \tag{3.2}$$

where $g_{K_A,max}$ is the maximum conductance of the channel given in Table 3.1, m_{ika} is the state variable of activation, and h_{ika} is the state variable of inactivation. The conductance of the potassium delayed rectifier channel is given by:

$$g_{k_{dr}} = g_{K_{dr},max} m_{ikdr}^4 \tag{3.3}$$

where $g_{K_{dr},max}$ is the maximum conductance of the channel given in Table 3.1 and m_{ikdr} is the state variable of activation. More detailed discussion of these channels can be found in (Safronov, Wolff, and Vogel, 2000). NEURON mod files for these

channels were obtained from Senselab model 138273[a]. Neurons were simulated at 37 °C using a timestep of 0.01 ms.

Table 3.1: Simple neuron ion channel conductances: the maximum conductances of the sodium channel ($g_{na,max}$), potassium fast channel ($g_{K_A,max}$), and potassium delayed rectifier channel ($g_{K_{dr},max}$) for each section type.

SectionType	$g_{na,max}$ (Ω^{-1} cm^{-2})	$g_{K_A,max}$ (Ω^{-1} cm^{-2})	$g_{K_{dr},max}$ (Ω^{-1} cm^{-2})
Soma	0.113	0.218	0.029
Proximal	0.003	0	0.001
Distal	0.003	0	0.001
AH	0.7	0	0.11
IS	0.7	0	0.11
AxonProper	0.012	0	0.04

From (Ostroumov, 2007)

3.2 Model neuron physical geometry

Detailed 3D models of neurons in the rat spinal cord are still very limited. Some researchers (Capogrosso et al., 2013) use the dendritic tree and soma from cat spinal neurons after resizing it and adding an axon. That is one possible solution, but it is unclear how similar these neurons are to the neurons in the rat spinal cord. More complex neuron models also require more computational resources. I chose to instead construct a simple neuron with parameters approximately matching those of (Thurbon et al., 1998) and (Ostroumov, 2007). It is my hope that using this simple neuron model at many locations, orientations, and stimulation configurations will compensate for the lack of a more complex model and perhaps give more general results.

Based on the morphological data in (Thurbon et al., 1998) the mean number of neurites in ventral horn neurons is 5.50 with sampled range from 3 to 8. Without additional data, I am assuming that the distribution in the dorsal horn is about the same and picking 6 neurites for the model. This also makes it easy to distribute

[a] https://senselab.med.yale.edu/modeldb/ShowModel.cshtml?model=138273&file=/NeuroMorph/Motoneuron-MorphoLogy/neuron/

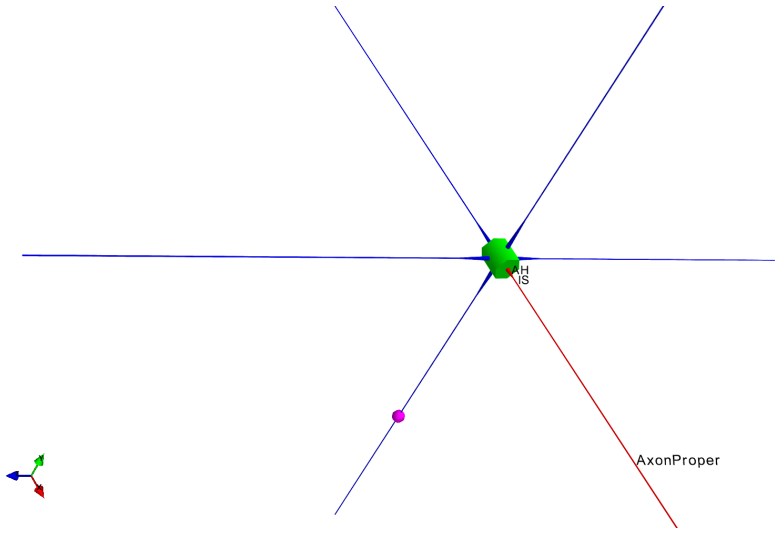

Figure 3.2: Model neuron showing dendrites (blue), soma (green), axon (red), and synapse location (pink ball). The synapse is shown here in the middle of one of the distal sections of the dendrites. This is one of the 5 possible location "A"s indicated in Fig. 3.3.

the neurites along the 6 Euclidean axis directions ($-\hat{x}$, $+\hat{x}$, $-\hat{y}$, $+\hat{y}$, $-\hat{z}$, and $+\hat{z}$) in an x-y-z coordinate system as described in Section 2.1.1. Based on the soma surface areas in (Thurbon et al., 1998), the mean spherical soma equivalent has a diameter of 25 µm and a range from 15.8 µm to 31.8 µm. A soma diameter of 20 µm was chosen to be in this range and match the model used in Table 2 of (Ostroumov, 2007). The total length of each neurite was chosen to be 290 µm to be approximately consistent with Figure 6 in (Thurbon et al., 1998). This means that each neuron fits inside a sphere with radius 300 µm.

The axon was modeled as 3 sections (listed proximal-distal from the soma), an axon hillock (AH) (with length 8 µm and a diameter varying linearly from 3 µm at the soma to 0.8 µm on the distal end), an initial segment (IS) (with a length of 10 µm and a constant diameter of 0.8 µm), and the axon proper (with a length of 272 µm[b] and a constant diameter of 0.8 µm). All of the axon parameters were taken from (Ostroumov, 2007) Section 3.2 except for the axon proper length which was chosen

[b] $(300 - 20/2 - 8 - 10)\mu m$

to match the total neurite size. The width of the axon is also supported by (Nunes et al., 2017; Saliani et al., 2017).

Each dendrite in the model consists of a proximal section (with length 25 µm, from Ostroumov 2007, Section 3.5) and a diameter varying linearly from 3 µm (consistent with AH diam and Ostroumov 2007 fig 2 (c) (1 dendritic end branch)) at the soma to 0.8 µm on the distal end) and a distal section (with length 265 µm[c] and constant diameter of 0.8 µm). The diameter of the distal section of the dendrite was selected based on the average diameter of a dendrite ((0.78 ± 0.05) µm) in (Thurbon et al., 1998) Table 3. The average diameter of a dendrite was calculated using $\frac{A_D}{\pi l_{Tot}}$ where A_D is the total membrane surface area in µm^2 and l_{Tot} is the total dendritic path length in µm. The physical parameters for this simple neuron are summarized in Table 3.2.

The total surface area for the soma (1256.6 µm^2), axon (823.1 µm^2), and dendrites (4115.5 µm^2) are in the distribution indicated in the sampling of neurons given in (Thurbon et al., 1998) Table 3.

Using the "d_lambda" rule from (M. L. Hines and N. T. Carnevale, 2001) and found at https://www.neuron.yale.edu/neuron/static/docs/d_lambda/d_lambda.html, the number of compartmental segments for the soma, proximal dendrite, axon hillock, and initial segment sections were each respectively set to 1. Similarly, the distal dendrites and the axon proper sections were set to have 17 segments. Please note that in this thesis, segments are numbered starting at 0, so the segments in the Distal dendrite or the AxonProper would be numbered [0, 1, 2, 3, 4, 5, 6, 7, 8, 9, 10, 11, 12, 13, 14, 15, 16], where segment 0 is closest to the soma, segment 8 is in the middle of the section, and segment 16 is at the distal tip.

[c] (300 − 20/2 − 25)µm

Table 3.2: Simple neuron physical parameters

SectionType	length (μm)	proximal diam (μm)	distal diam (μm)
soma	20	20	20
proximal dendrite	25*	3†	0.8‡
distal dendrite	265§	0.8‡	0.8‡
axon hillock	8¶	3¶	0.8‡
IS	10¶	0.8‡	0.8‡
AxonProper	272‖	0.8¶	0.8¶

* (Ostroumov, 2007) Section 3.5
† Consistent with AH and (Ostroumov, 2007) fig 2 (c) (1 dendritic end branch)
‡ Calculated from Thurbon 1998 Table 3 using average diameter of a dendrite = $\frac{A_D}{\pi l_{Tot}}$ where A_D is the total membrane surface area in μm^2, and l_{Tot} is the total dendritic path length in μm. The average diameter of a dendrite was (0.78 ± 0.18) μm.
§ 300 − 20/2 − 25
¶ (Ostroumov, 2007) Section 3.2 also consistent with ‡ and (Nunes et al., 2017)
‖ 300 − 20/2 − 8 − 10

Table 3.3: Simple neuron segments based on "d_lambda" rule from (M. L. Hines and N. T. Carnevale, 2001)

SectionType	number of segments
Soma	1
Proximal	1
Distal	17
AH	1
IS	1
AxonProper	17

3.3 Neurotransmitter models

In a biological neural system, information enters a post-synaptic neuron when a pre-synaptic neuron releases neurotransmitters which bind to ligand-gated ion channels on the post-synaptic neuron. The ligand-gated ion channels then open and cause a post-synaptic potential (PSP). In the case of an excitatory synapse, this is referred to as an excitatory post-synaptic potential (EPSP). If the sum of the PSPs (both inhibitory and excitatory) in the neuron increases the potential above a certain threshold value, an action potential occurs. If the action potential reaches the

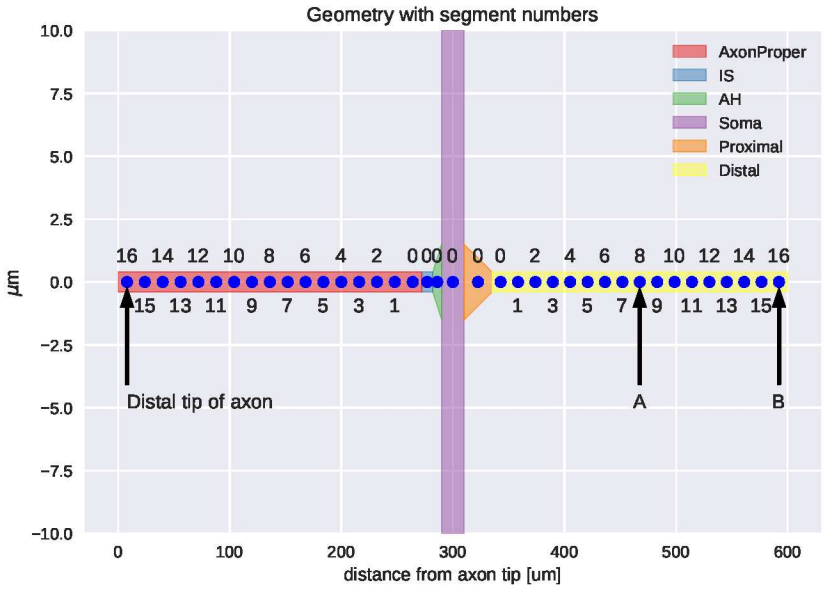

Figure 3.3: This figure shows the sections of the model neuron from the axon tip on the left side to the distal tip of one of the dendrites on the right side. Only one of the 5 dendrites is shown (since the rest only differ in orientation). Each section type is labeled by color (see legend). The diameter of the various sections is indicated by the size of the section on the vertical axis and the length of each section on the horizontal axis. The horizontal axis also indicates the path length distance from the axon tip. The center of each segment inside each section is indicated by a blue circle and labeled with a black number. The distal tip of the axon is labeled. Location "A" is in the middle of the distal section of the dendrite with segment number 8. Location "B" is at the distal tip of the distal section of the dendrite with segment number 16. These locations will be used for probe points in Chapters 3 to 5 and synapse locations in Chapters 3 and 5. Note that because there are 5 dendrites, there are 5 location "A"s and 5 location "B"s on each neuron. These will be distinguished (if it matters) by indicating the orientation of the dendrite the location is on. See Fig. 3.2 for a 3D view of the entire neuron.

axon tip, usually the membrane voltage at the axon tip is raised sufficiently for neurotransmitters to be released from the axon tip and communicate with the next cell.

Studying the facilitation of information transmission in neurons requires models for the synaptic current generated when the neurotransmitters are received, the neuron processes the input, and neurotransmitter is released.

3.3.1 Synapse model: Exp2Syn

The current through a synapse after the synapse is triggered by neurotransmitters from the presynaptic cell was modeled using the Exp2Syn[d] synapse model. The Exp2Syn consists of a trans-membrane current (Santos et al., 2009):

$$I_{syn} = g_{syn} * (V_{m@syn} - E_{\text{Rev}}) \tag{3.4}$$

where

$$g_{syn} = \frac{\tau_D}{\tau_D - \tau_R} * (e^{\frac{-t}{\tau_D}} - e^{\frac{-t}{\tau_R}}) * g_M, \tag{3.5}$$

τ_D is the conductance decay time constant, τ_R is the conductance rise time constant, g_M is the maximum synapse conductance (also referred to as the synaptic weight), V_m is the membrane voltage at the synapse location, and E_{Rev} is the reversal potential. In this thesis, $\tau_R = 0.5\,\text{ms}$, $\tau_D = 5\,\text{ms}$, and $E_{\text{Rev}} = 0$. These values correspond to excitatory glutamatergic synapses formed by interneurons in the substantia gelatinosa in the rat spinal cord and were obtained from (Santos et al., 2009).

Each time that an excitatory synapse is triggered (by neurotransmitters from a presynaptic neuron in a real biological system or by a trigger event in simulation) the time-varying trans-membrane current I_{syn} gives rise to a change in the membrane voltage at the synapse and the rest of the cell. As mentioned previously, this change in membrane voltage is referred to as an excitatory post-synaptic potential or EPSP. Each EPSP depends indirectly on the entire state of the neuron, since the tran-membrane current (I_{syn}) is dependent on the membrane current at the synapse ($V_{m@syn}$). $V_{m@syn}$ is in turn dependent (indirectly) on the state of the entire neuron (V_m, V_e, and ion channel states). One or more of these EPSPs can combine to

[d] https://www.neuron.yale.edu/neuron/static/py_doc/modelspec/programmatic/mechanisms/mech.html#Exp2Syn

cause enough of an increase in the membrane potential at the axon tip to activate the neuron and cause the release of neurotransmitters.

3.3.2 Neurotransmitter release

Most other stimulation literature uses recruitment/activation definitions similar to "considered recruited if the resulting depolarization elicited an action potential that traveled along the efferent axon" (Capogrosso et al., 2013) or "propagating action potentials were initiated" (J Ladenbauer et al., 2010). Unfortunately, when dealing with electrical stimulation of neurons, these definitions can be ambiguous. For example, an action potential may be generated near the soma but not reach the axon tip with sufficient potential to cause neurotransmitter release because the external stimulating field can quench activity further down the axon. The opposite can also occur, where no action potential is generated but the membrane voltage at the axon tip is raised by stimulation above the amount necessary to release neurotransmitters. For information to be transmitted to the next post-synaptic neuron, the release of neurotransmitters is required, while action potentials may not be.

While neurotransmitter release could be modeled using kinetic models as in (Destexhe, Mainen, and Sejnowski, 1994), this thesis study uses Equation (37) from (Destexhe, Mainen, and Sejnowski, 1994) to model this process:

$$[L](V_{pre}) = \frac{L_{\max}}{1 + \exp(-(V_{pre} - V_p)/K_p)} \tag{3.6}$$

where $[L]$ is the concentration of an arbitrary neurotransmitter L, V_{pre} is the presynaptic membrane voltage measured in the axon tip, $L_{\max} = 2.84\,\text{mM}$ is the maximum concentration of neurotransmitter in the synaptic cleft, $V_p = 2\,\text{mV}$, and $K_p = 5\,\text{mV}$. This equation is plotted in Fig. 3.4. For the purposes of this thesis, a neuron is considered to have released neurotransmitters if the membrane voltage on the distal tip of the axon goes above $-10\,\text{mV}$, and in this case, will be referred to as

an *active* neuron.

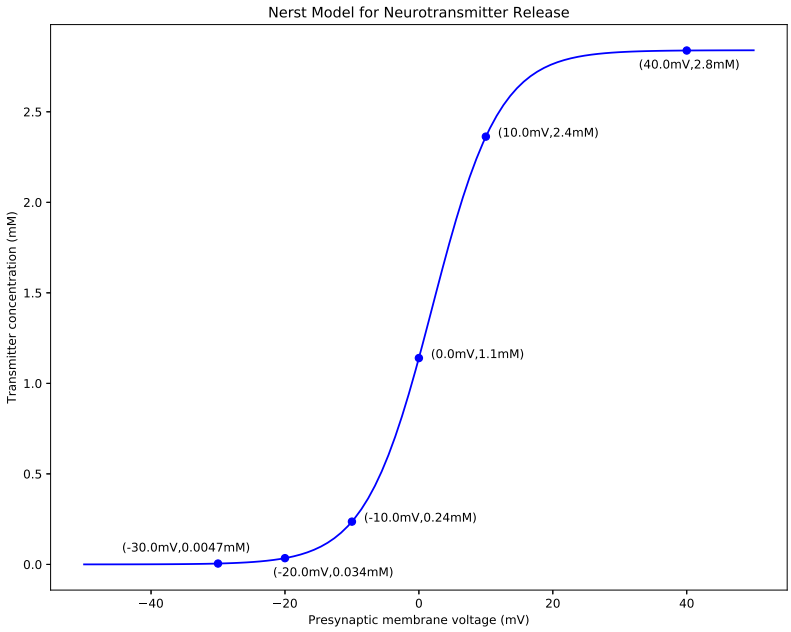

Figure 3.4: Amount of neurotransmitter released (in millimolar concentration) as a function of membrane voltage (in mV) from Eq. (3.6).

3.4 Neuron characterization

In order to better understand the behavior of the simple neuron model and to benchmark the model against other known results, computational experiments were conducted to determine the resting potential, the firing threshold of the neuron in response to current pulse injection, and the firing threshold in response to synapse firing.

3.4.1 Resting potential of model neuron

Six neuron models were generated with their axons lying respectively along the $-\hat{x}$, $+\hat{x}$, $-\hat{y}$, $+\hat{y}$, $-\hat{z}$, and $+\hat{z}$ directions, i.e. an axon located along the $+\hat{x}$ direction has its distal tip located in a more positive x-coordinate than the soma. The initial membrane voltage (V_m) in all segments of all sections of the neurons was set to

$v_{init} = -70\,\text{mV}$ at $t = 0$. Then a NEURON simulation is executed for 800 ms (without an external electric field or synapses firing) until the simulated neuron's membrane voltage reaches steady state. The state of each neuron model at steady state was saved so that it could be reloaded to save computational time for future simulations. The resting membrane voltage at the end of these simulations can be seen in Fig. 3.5.

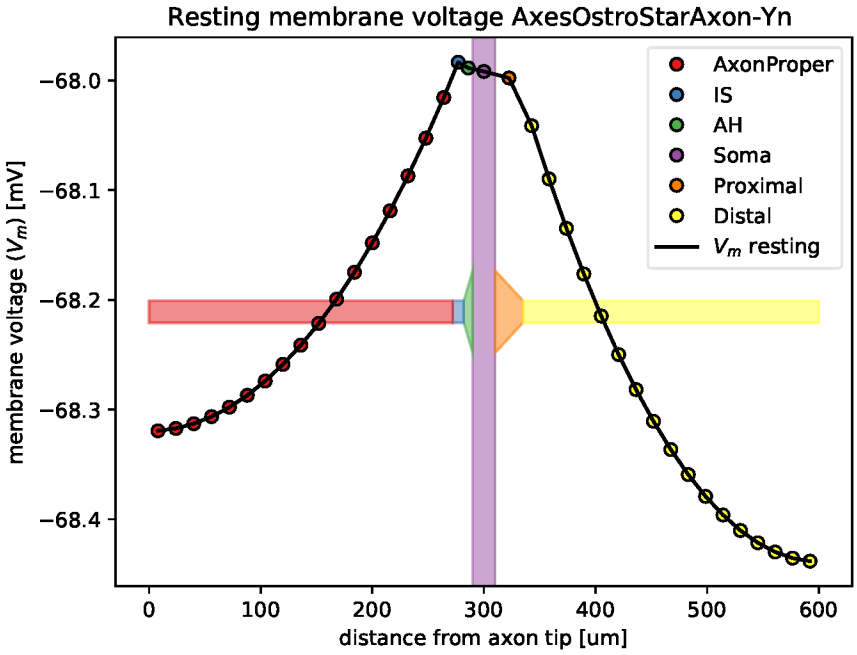

Figure 3.5: The resting membrane voltage (V_m) for each segment along the model neuron's axon, soma, and a single dendrite after 800 ms of simulation time with no external inputs. The colored polygons show where the neuron model sections are and their relative diameters. Since all five dendrites in the model have an identical resting membrane voltage distribution as a function of distance from the soma, only one result is plotted.

3.4.2 Current injection

One way to validate the neuron model used in this thesis is to compare the response of the neuron to a known experimental configuration used in other papers. The (Ostroumov, 2007) paper contains 2 current injection studies where increasing amplitudes of square current pulses (width = 0.1 ms in Figure 4(c) and width 5 ms in Figure 4(d)[e]) are injected into the soma until one of them causes the membrane voltage at the soma to exceed -10 mV. The results for the simple neuron model, a modified simple neuron model with thicker dendrites, and the data from (Ostroumov, 2007) are summarized in Table 3.4. The model presented in (Ostroumov, 2007) requires between 2.4 to 2.95 times more current for a 5 ms pulse and 3 to 4.3 times more current for a 0.1 ms pulse compared with the simple model presented in this chapter. As seen in Table 3.4, the simple model used in this thesis has a smaller surface area than the model neuron presented in (Ostroumov, 2007). In order to see how much these thresholds depend on the surface area of the dendrites, a modified model neuron was created with the diameter of the distal dendrites increased by a factor of 2 (so that the diameter is now 1.6 µm). With this change, the (Ostroumov, 2007) model requires 1-1.11 times the current for the 5 ms pulse and 1.3-1.8 for the 0.1 ms pulse compared with the modified simple neuron model. Note that the wide range of scale factors presented here is due to the lack of specificity in the threshold values in (Ostroumov, 2007). It appears based on this test that the additional current required to reach threshold can be explained by the increased surface area of the Ostroumov model. Since neurons with smaller and larger surface areas have been found in the rat spinal cord (see Table 3 in (Thurbon et al., 1998)), it appears based on this test that the simple model neuron used in this thesis has properties similar to neurons in the rat spinal cord.

[e]Note that unfortunately (Ostroumov, 2007) Figure 4(c) incorrectly labels the current pulses in mA instead of µA, and Figure 4(d) incorrectly shows amplitude of the current pulse as 5 nA instead of 0.5 nA as described in the caption.

Additional plots and discussion of the effects of current injection can be found in Section 3.A.

Table 3.4: Current injection thresholds necessary for a current pulse with a width of 0.1 ms (⎍ column) or 5 ms (⎍ column) injected into the soma to cause the soma's membrane voltage to exceed −10 mV. Three neuron models are presented: the simple neuron model used in the rest of the thesis, a modified version of the simple neuron with dendrites that are twice as thick, and the data from (Ostroumov, 2007) for comparison. Columns A_S, A_A, and A_D are the surface area of the soma, axon, and all the dendrites respectively.

Model	A_S (μm^2)	A_A (μm^2)	A_D (μm^2)	0.1 ms ⎍ threshold*	5 ms ⎍ threshold*
Simple	1256.6	823.1	4115.5	6.944nA	0.169nA
Simple with distal dendrite diam=1.6 μm	1256.6	823.1	7759.7	15.929nA	0.447nA
(Ostroumov, 2007) model	1305 ± 21	1350†	7514 ± 74	30nA	0.5nA

* Amplitude of current pulse required to for the membrane voltage at the soma to exceed −10 mV.
† Calculated based on an axon 500 μm long with the parameters in the paper.
For the thresholds calculated using the simple neuron model and the modified simple neuron model, reducing the value given in the table by 0.001 nA causes the membrane voltage at the soma to be less then −10 mV.

3.4.3 Synapse Thresholds

In a real biological system without electrical stimulation, one or more EPSPs from one or more synapses would combine to trigger an action potential. There is little data on the maximum conductance (g_M) of synapses in the rat spinal cord. Santos et al. (2009) use values between 0.02 nS and 0.23 nS without reference to actual measurements. In order to simplify the facilitation study in Chapter 5, I have assumed that either some neurons exist in the spinal cord with synapses with near threshold weights or that multiple active synapses (perhaps with highly synchronous input) resulting in a near threshold potential can be approximated by a single near threshold potential.

I used linear extrapolation combined with a binary search to bracket the synapse weights necessary for a single synapse positioned at locations from the soma to the distal tip of a dendrite to cause the membrane voltage at the axon tip to just exceed values −60 mV to 10 mV in steps of 10 mV. The results of this search can be seen in Fig. 3.6. The difference in synapse weight to achieve a membrane voltage of −50 mV is very close to that needed to achieve 0 mV. For the synapse weights found and shown in Fig. 3.6, Fig. 3.7 shows the amount of time necessary for the axon tip membrane voltage to reach the target voltage. Signals with a peak membrane

voltage at the axon tip of $-20\,\text{mV}$, $-30\,\text{mV}$, and $-40\,\text{mV}$ take the longest time for the peak of the signal to reach the axon tip.

The membrane voltage at the axon tip as a function of synaptic weight for synapses located at the middle and distal tip of the distal dendrite section can be found in Figs. 3.8 and 3.11 respectively. Specific sub-threshold synapse weights have been marked with red vertical lines on these figures for use in the facilitation studies in Chapter 5. The largest selected synapse weights can also be seen in Figs. 3.9 and 3.12, which are close ups of Figs. 3.8 and 3.11. These figures also show that very small differences in synapse weight can cause the axon tip membrane voltage to increase from $-50\,\text{mV}$ to $0\,\text{mV}$.

The response of the neuron (membrane voltage and ion-channel state variables) to input at a synapse located in the middle of the distal dendrite section when triggered with synapse weight of $3.45\,\text{nS}$ can be found in Fig. 3.10. A similar plot for a synapse located at the distal dendrite tip with synapse weight of $4.783\,\text{nS}$ can be found in Fig. 3.13. These plots are provided for comparison to similar plots in Chapters 4 and 5.

Synapse weight thresholds for membrane voltages on the soma are presented in Section 3.B for possible comparison with soma patch clamp data.

Additional simulations with passive dendrites, active dendrites with double the diameter, and passive dendrites with an axon with double the diameter all required a larger synapse weight to cause neurotransmitter release. Simulations with passive dendrites required significantly larger synaptic weights.

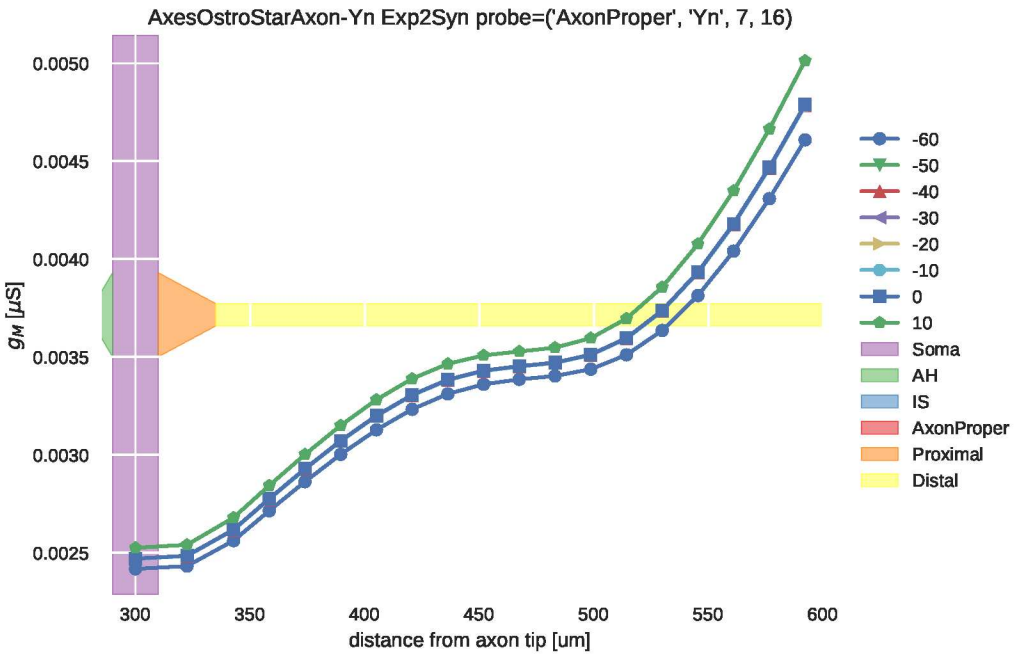

Figure 3.6: Synapse weight (g_M) (y-axis in µS) necessary for a synapse at that distance (x-axis in µm) from the axon tip to cause the specified membrane voltage (see legend: −60 mV to 10 mV in steps of 10 mV) at the axon tip after a single synapse event. Note that as the synapse location is farther from the soma, the synapse weight necessary to cause a given membrane voltage at the axon tip increases. Lines and symbols for −50 mV through 0 mV are plotted on top of each other.

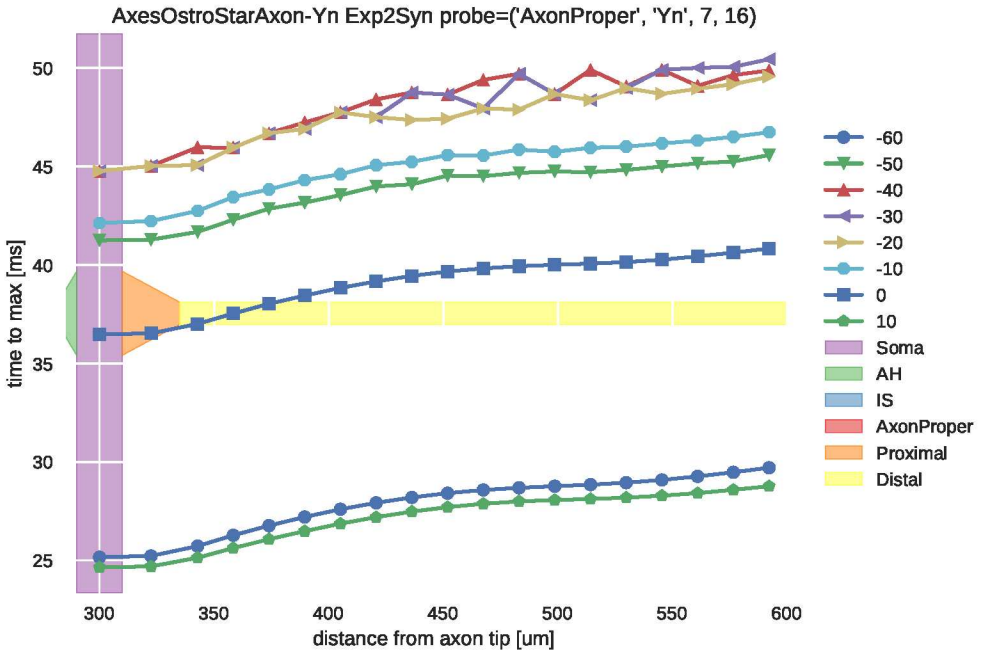

Figure 3.7: The time required for the axon tip to reach maximum membrane voltage (y-axis in µs) when a synapse triggered at that distance from the axon tip (x-axis) with the synapse weight necessary (see Fig. 3.6) to reach the specified membrane voltage (see legend) is triggered.

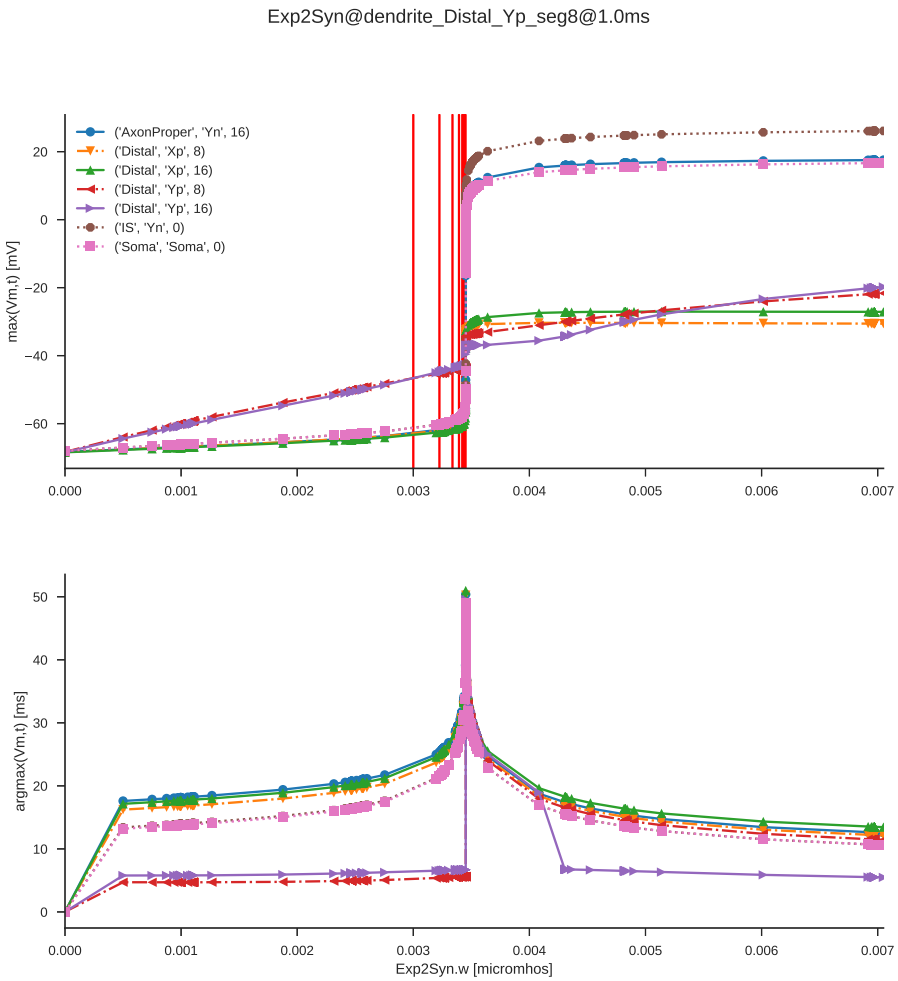

Figure 3.8: Maximum membrane voltage (top) and time to reach that maximum (from simulation start (synapse fire starts at 1ms)) (bottom) at probe locations (see legend) in the neuron when a synapse fires in the middle of the distal section of one of the dendrites. Red vertical lines mark synapse weight values ([3.45, 3.443, 3.436, 3.422, 3.394, 3.337, 3.225, and 3] nS) used for facilitation in Chapter 5. Top and bottom plots share the same x-axis.

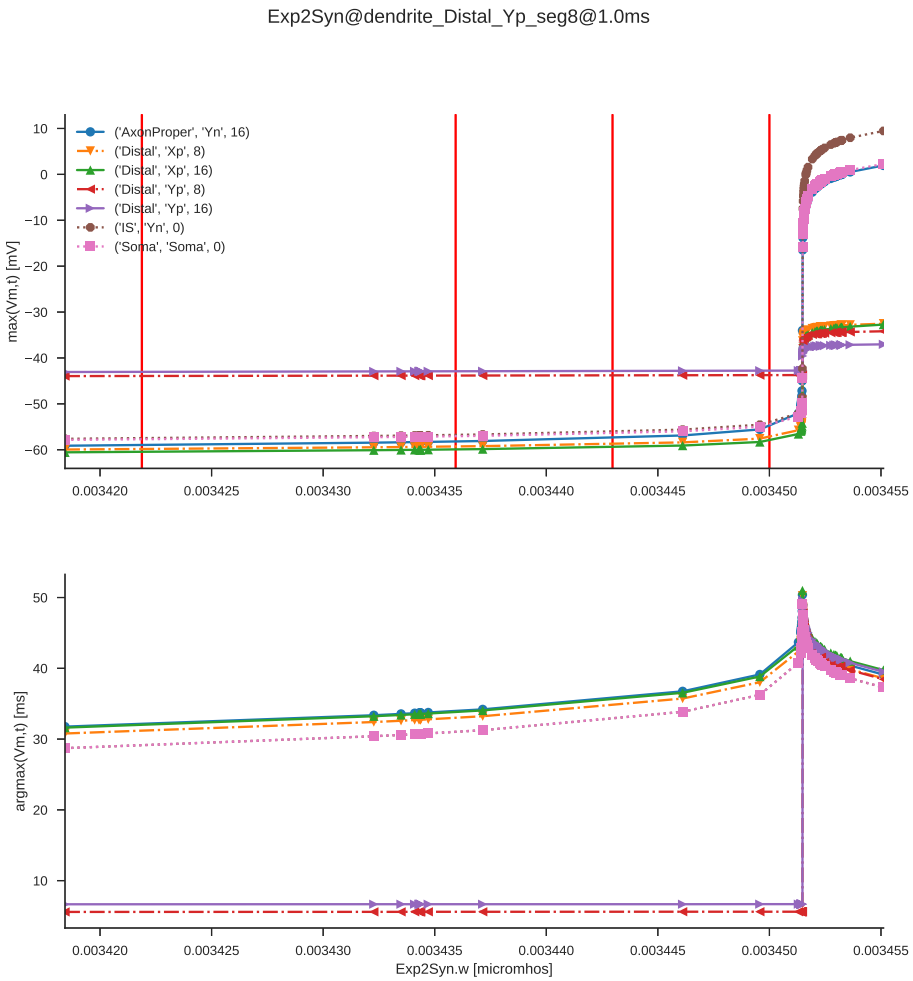

Figure 3.9: A close up of Fig. 3.8 showing the largest 4 facilitation synapse weights. Maximum membrane voltage (top) and time to reach that maximum (from simulation start (synapse fire starts at 1ms)) (bottom) at probe locations (see legend) in the neuron when a synapse fires in the middle of the distal section of one of the dendrites. Red vertical lines mark synapse weight values ([3.45, 3.443, 3.436, 3.422] nS) used for facilitation in Chapter 5.

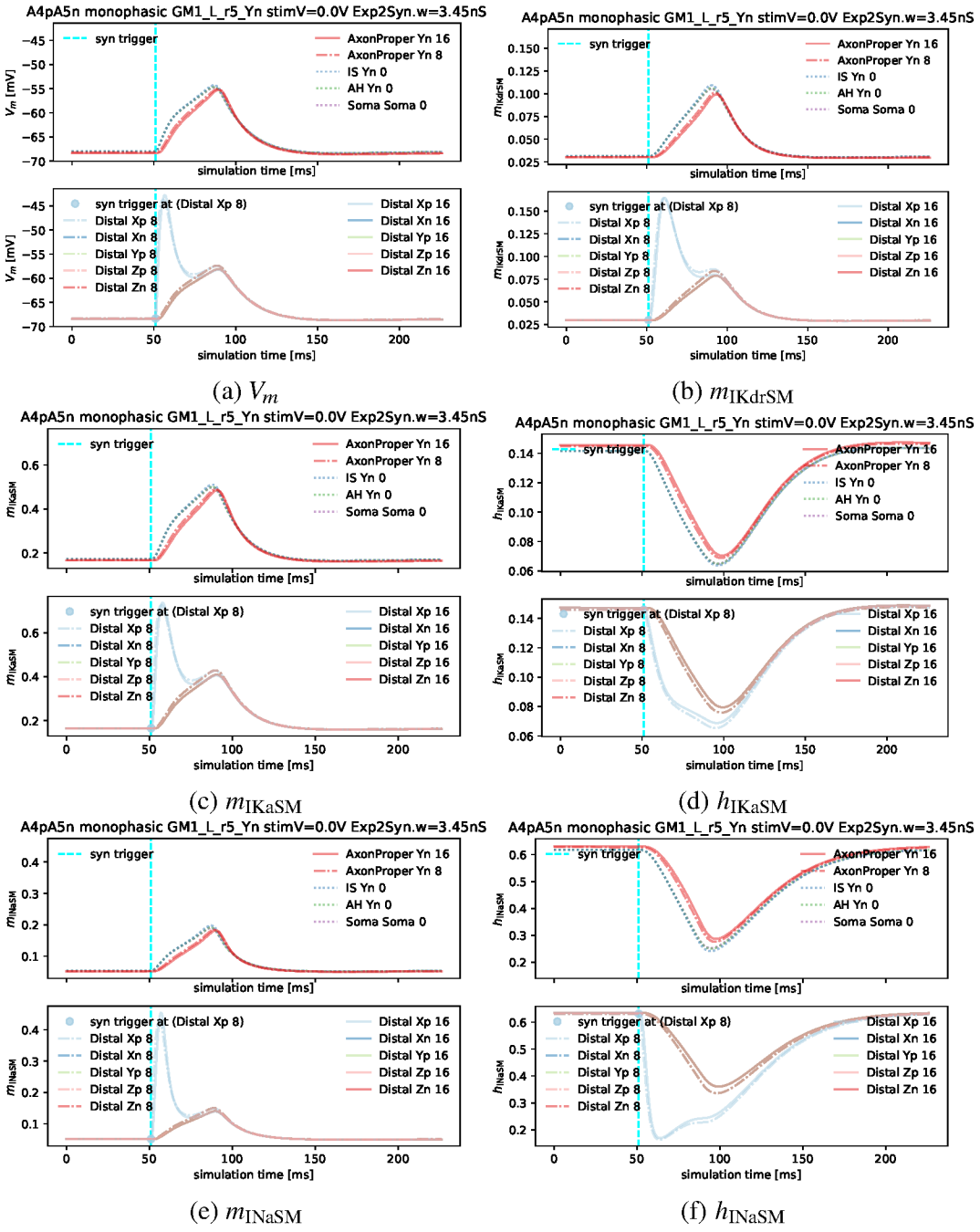

(a) V_m (b) m_{IKdrSM}

(c) m_{IKaSM} (d) h_{IKaSM}

(e) m_{INaSM} (f) h_{INaSM}

Figure 3.10: Time series of the internal state of the neuron model after a single EPSP was triggered at a synapse located in the middle of a distal dendrite section with a synaptic weight of 3.45 nS. Each subplot plots a different variable ((a) V_m, (b) m_{IKdrSM}, (c) m_{IKaSM}, (d) h_{IKaSM}, (e) m_{INaSM}, and (f) h_{INaSM}) against simulation time (ms) for probes on axon-soma (a through f top) and dendrites (a through f bottom).

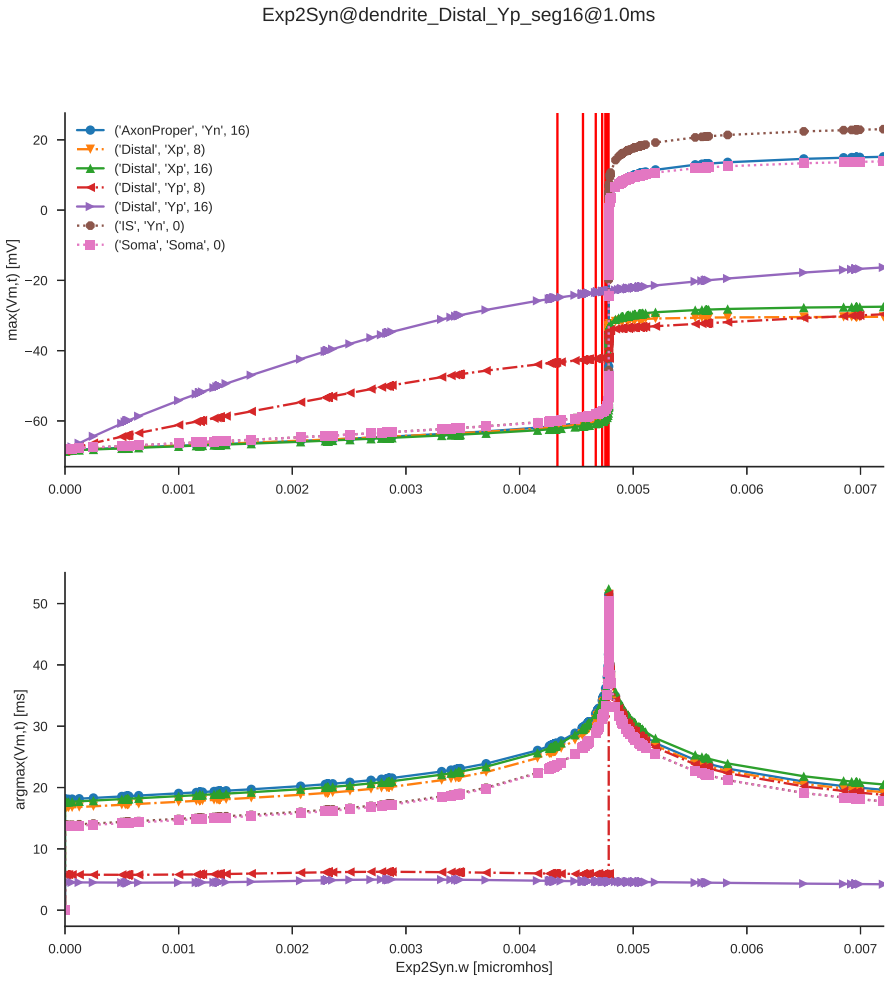

Figure 3.11: Maximum membrane voltage (top) and time to reach that maximum (from simulation start (synapse fire starts at 1ms)) (bottom) at probe locations (see legend) in the neuron when a synapse fires at the distal tip of one of the dendrites. Red vertical lines mark synapse weight values ([4.783, 4.776, and 4.769] nS) used for facilitation in Chapter 5. Top and bottom plots share the same x-axis.

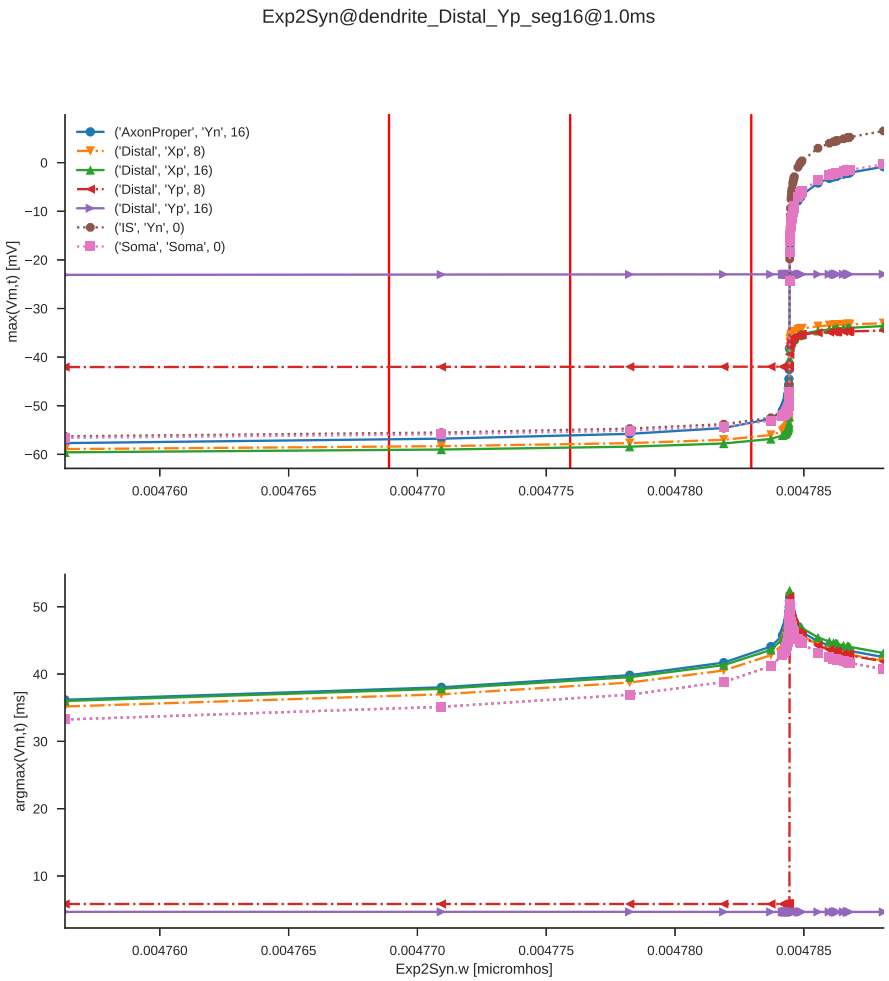

Figure 3.12: A close up of Fig. 3.11 showing the largest 3 facilitation synapse weights. Maximum membrane voltage (top) and time to reach that maximum (from simulation start (synapse fire starts at 1ms)) (bottom) at probe locations (see legend) in the neuron when a synapse fires at the distal tip of one of the dendrites. Red vertical lines mark synapse weight values ([4.783, 4.776, and 4.769] nS) used for facilitation in Chapter 5.

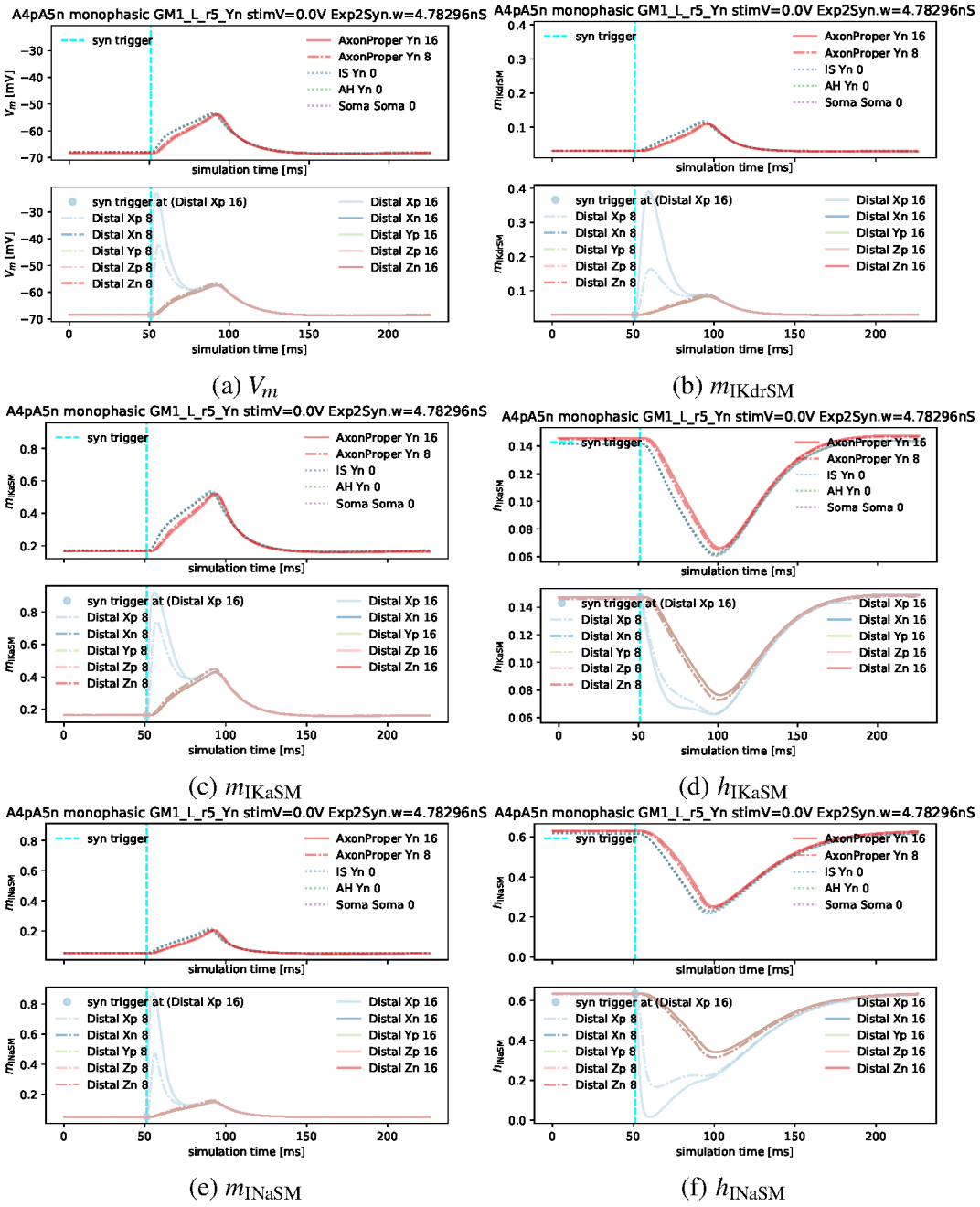

(a) V_m (b) m_{IKdrSM}

(c) m_{IKaSM} (d) h_{IKaSM}

(e) m_{INaSM} (f) h_{INaSM}

Figure 3.13: Time series of the internal state of the neuron model after a single EPSP was triggered at a synapse located at the distal tip of a dendrite with a weight of 4.78 nS. Each subplot plots a different variable ((a) V_m, (b) m_{IKdrSM}, (c) m_{IKaSM}, (d) h_{IKaSM}, (e) m_{INaSM}, and (f) h_{INaSM}) against simulation time (ms) for probes on axon-soma (a through f top) and dendrites (a through f bottom).

3.5 Error discussion

It is important to try to quantify the possible sources of errors in any experiment or simulation. Based on the modeling methods introduced in Chapters 2 and 3, I can divide the possible sources of error into geometric errors, biophysical parameter errors, and numerical computational errors.

There are a number of these possible types of errors in the volume conductor model. Although I used a transverse slice from an MRI of a rat spine as the basis for the model extrusion, the detailed segmental variations in the lumbosacral spinal cord were not taken into account. None of the issues studied in this thesis are dependent upon specific properties or functions of particular spinal segments. The electrode array used in these simulations is based on an actual array (Parag Gad, Choe, et al., 2013) used in rats, but placement in individual subjects might differ in minor ways.

A number of biophysical parameters are used in the volume conductor simulation. The conductivity and permittivity of the parylene C and platinum are known to a fairly high precision and are unlikely to change the results. For the tissues in the volume conductor model, I have collected the best frequency dependent values of conductivity and permittivity from multiple sources. Rarely is the frequency dependent nature of these parameters taken into account. Incorporating this frequency dependence should reduce the effective error in the simulated results, but the fact remains that these values are going to vary across subjects. Changes in these values would likely change the depth and shape of the electrical penetration in the spinal cord. These would likely cause minor differences in the stimulation thresholds (Chapter 4) and facilitation amounts (Chapter 5).

The volume conductor simulations depend on finite-element meshing techniques and computational approaches. Boundary effects in the model were tested in Section 2.2.1 and found to be minimal after avoiding rows 1 and 7. Boundary effects

with the electrode surfaces are believed to be minimal a small distance away from the electrodes and were also minimized by controlling the voltage of the back surface of the electrode rather than the front surface. Meshing errors are also possible, but were minimized by looking at the mesh quality as calculated by COMSOL and tested by comparing voltages for translated and reflected electrode combinations which should result in the same voltage potentials (Section 2.2.1).

My goal for the neuron model was not to study one particular neuron, but to use a nominal model whose surface area and size falls into the distribution of neurons in the rat spinal cord (Thurbon et al., 1998). That being said, it is possible that particular geometrical features not included in this model may react differently to stimulation. I have tried to minimize these effects by testing these neurons in many locations, orientations, and electrode combinations.

For the biophysical parameters of the neuron model, the key membrane biophysical parameters are membrane capacitance, membrane resistance, and the ion channel densities. While ion channel densities may vary across neuron types, the values that I selected were taken from studies based using mostly rat spinal neurons.

There may also be errors due to the compartmental modeling of the neurons. I have tried to address these issues by following the d_lambda rule (M. L. Hines and N. T. Carnevale, 2001).

In this model, I have assumed that the external electric field is not modified by the neurons. This assumption (while widely used) is not completely correct (Ye and Steiger, 2015) and may lead to minor errors.

I have tried to present the sources of errors here and the decisions taken to mitigate them. Since the errors in many of these parameters are not well understood, it is difficult to place precise error bars on the results of the ensuing chapters. The effects of these errors can be practically interpreted in terms of perturbations to

the electric and current density distributions in the volume conductor model. The use of many different neuron locations, orientations, and electrode combinations should minimize the effect of these errors on the interpretation of the results of these simulations.

The main point of this thesis is to show that facilitation of interneurons is possible under a variety of stimulating conditions. The subsequent chapters will find thresholds for activation and facilitation under a variety of stimulating conditions, and I believe that these errors would perturb these thresholds and only alter the spatial boundaries of the facilitation effect, and not the existence of this important phenomenon.

3.6 Summary

In this chapter, I described the electrical and geometrical properties of a model neuron that will be used in the rest of the thesis. The geometrical values (surface areas, diameters, number of neurites, etc.) are within the distribution of values for rat spinal cord neurons found in (Thurbon et al., 1998) Table 3. A study of current injection at the soma showed that less current was required compared to the model used in (Ostroumov, 2007), but that this decrease was likely due to the larger surface area of the Ostroumov model.

Rather than using the presence of action potentials on the axon, even for a brief time as a measure of neuron recruitment, I used the principle that neurons transmit information with the release of neurotransmitters from the axon tip. This principle in combination with the work of Destexhe and colleagues (Destexhe, Mainen, and Sejnowski, 1994) simplified the analysis and removed ambiguity. Based on this analysis, a neuron is judged to be active and to have released neurotransmitters if the membrane voltage at the axon tip exceeds $-10\,\mathrm{mV}$.

A synapse model was introduced, and sub-threshold weight values were found for

synapse locations at the middle and distal tip of the distal section of the dendrites. These will be used for the facilitation studies in Chapter 5.

3.A Appendix: Current injection

In Section 3.4.2, thresholds for a 0.1 ms and a 5 ms square current pulse were determined for comparison with (Ostroumov, 2007) and other papers. In this appendix, related figures for the 0.1 ms pulse are presented for reference. Please see the attached captions for explanations.

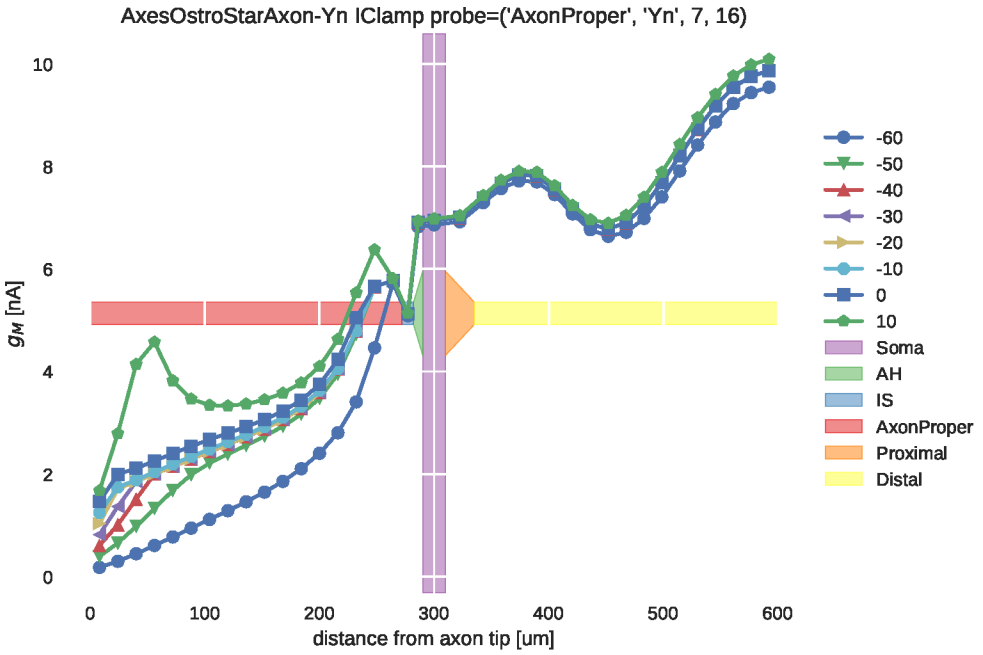

Figure 3.14: Current amplitude (y-axis in nA) necessary for a single square current pulse 0.1 ms long injected at that distance (x-axis in µm) from the axon tip to cause the specified membrane voltage (see legend: −60 mV to 10 mV in steps of 10 mV) at the axon tip.

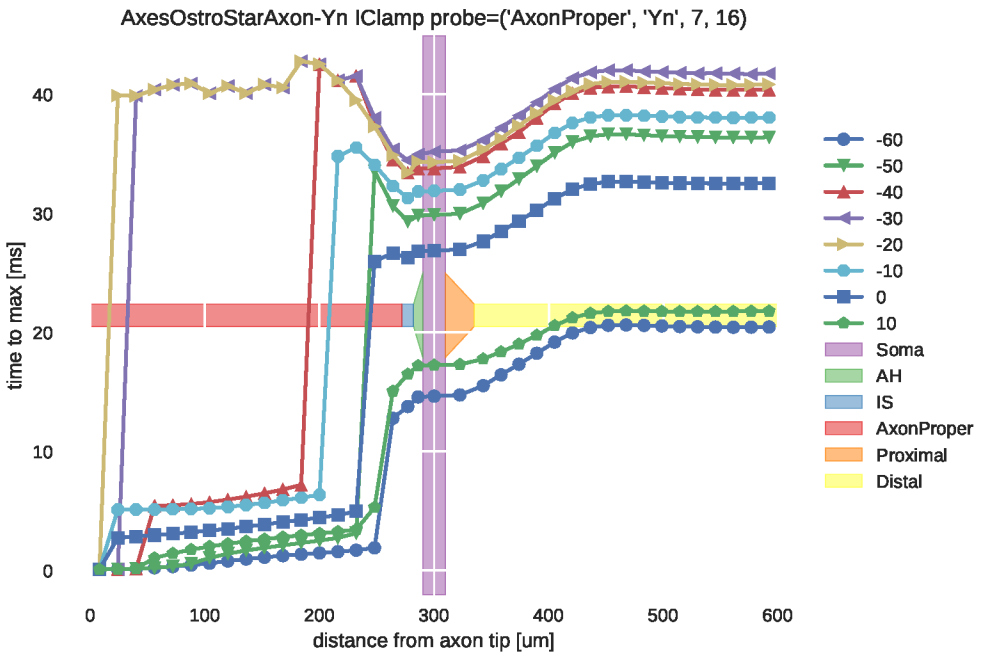

Figure 3.15: The time required for the axon tip to reach maximum membrane voltage (y-axis in µs) when a 0.1 ms square current pulse is injected at that distance from the axon tip (x-axis) with the current necessary (see Fig. 3.6) to reach the specified membrane voltage (see legend).

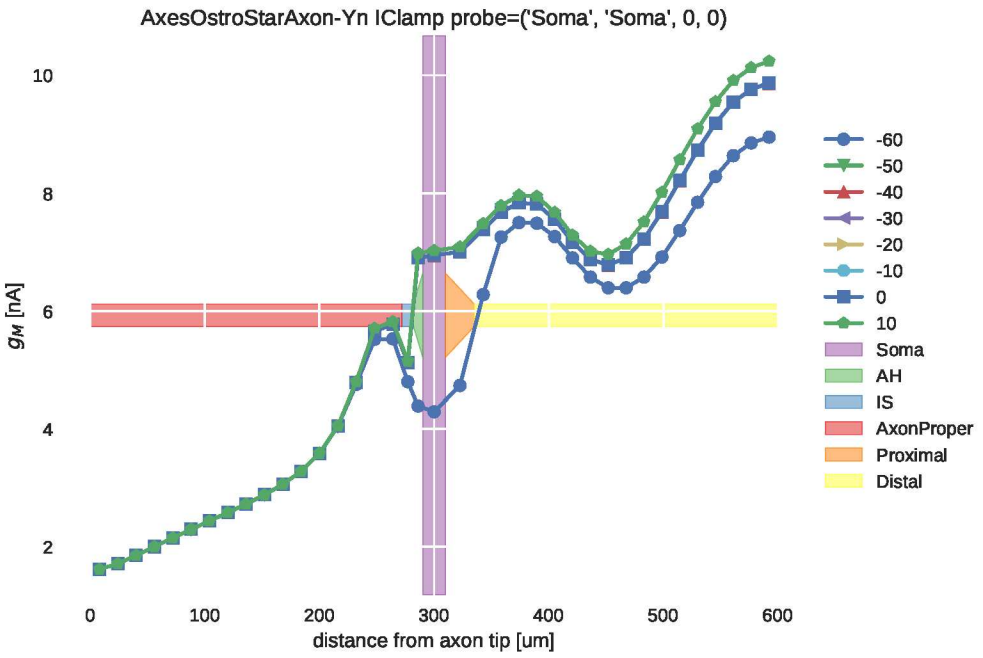

Figure 3.16: Current amplitude (y-axis in nA) necessary for a single square current pulse 0.1 ms long injected at that distance (x-axis in µm) from the axon tip to cause the specified membrane voltage (see legend: −60 mV to 10 mV in steps of 10 mV) at the soma.

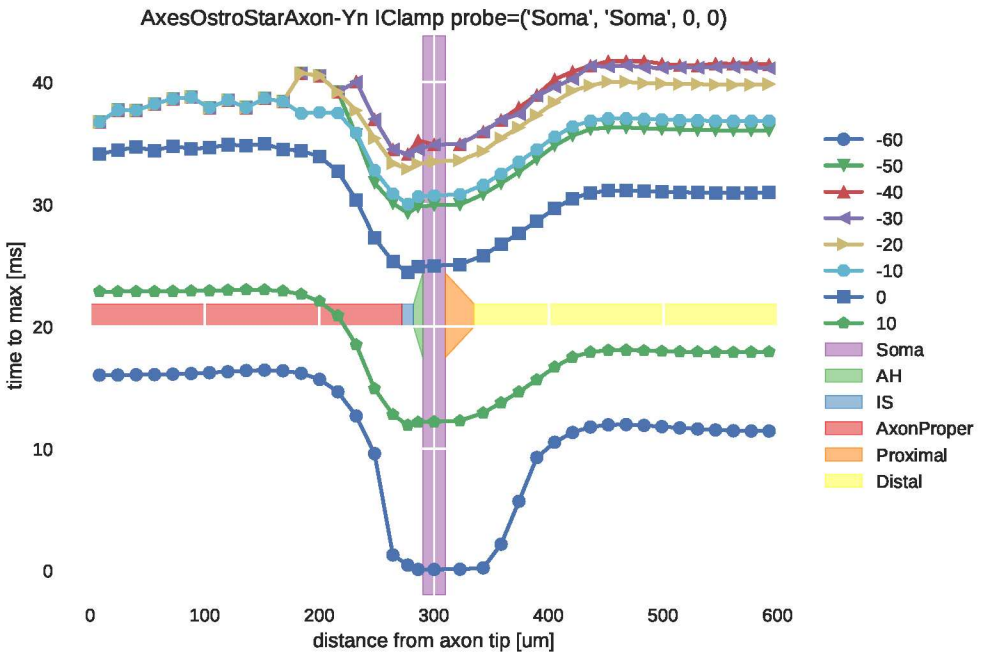

Figure 3.17: The time required for the soma to reach maximum membrane voltage (y-axis in µs) when a 0.1 ms square current pulse is injected at that distance from the axon tip (x-axis) with the current necessary (see Fig. 3.16) to reach the specified membrane voltage (see legend).

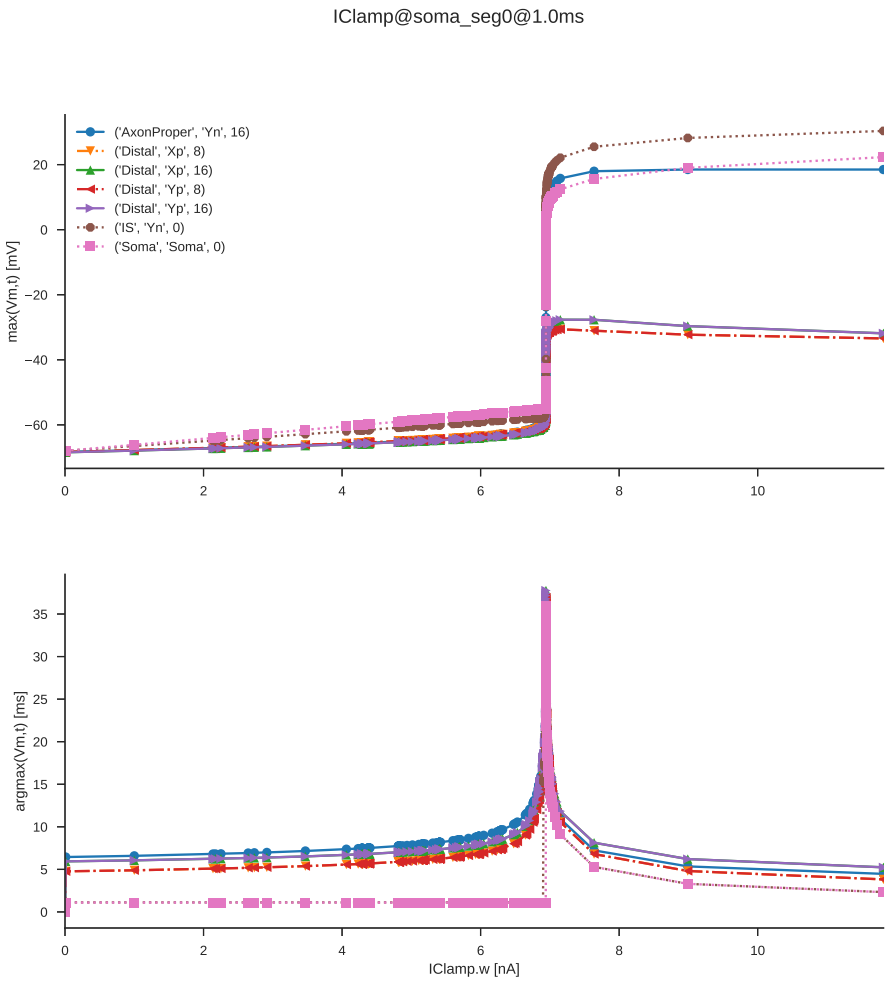

Figure 3.18: Maximum membrane voltage vs the amplitude of a 0.1 ms square current pulse injected at the soma (top) and time to reach that maximum (from simulation start (pulse occurs at 1ms)) vs injected current (bottom). Each colored line corresponds to a probe location labeled by (section type, axis direction, segment number). This figure corresponds to the threshold of 6.944nA for the simple neuron model given in Table 3.4.

3.B Appendix: synapse thresholds at the soma for comparison

It is usually easier to measure the membrane voltage of a real neuron at the soma rather than at the distal tip of an axon. For that reason, I repeated the analysis given in Section 3.4.3 for soma membrane voltages of −60 mV to 10 mV in steps of 10 mV. Again, linear extrapolation combined with a binary search was used to bracket the synapse weights necessary for a single synapse located at locations from the soma to the distal tip of a dendrite to cause the membrane voltage at the soma to just exceed the specified membrane voltages.

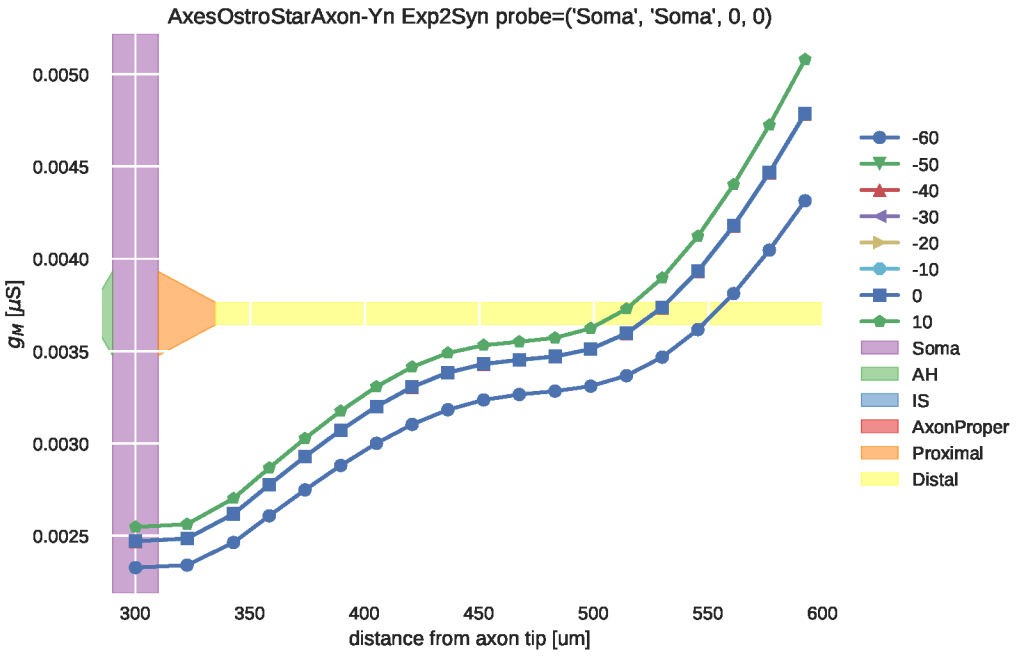

Figure 3.19: Synapse weight (g_M) (y-axis in µS) necessary for a synapse at that distance (x-axis in µm) from the axon tip to cause the specified membrane voltage (see legend: −60 mV to 10 mV in steps of 10 mV) at the soma after a single synapse event. Note that as the synapse location is farther from the soma, the synapse weight necessary to cause a given membrane voltage at the soma increases. Lines and symbols for −50 mV through 0 mV are plotted on top of each other.

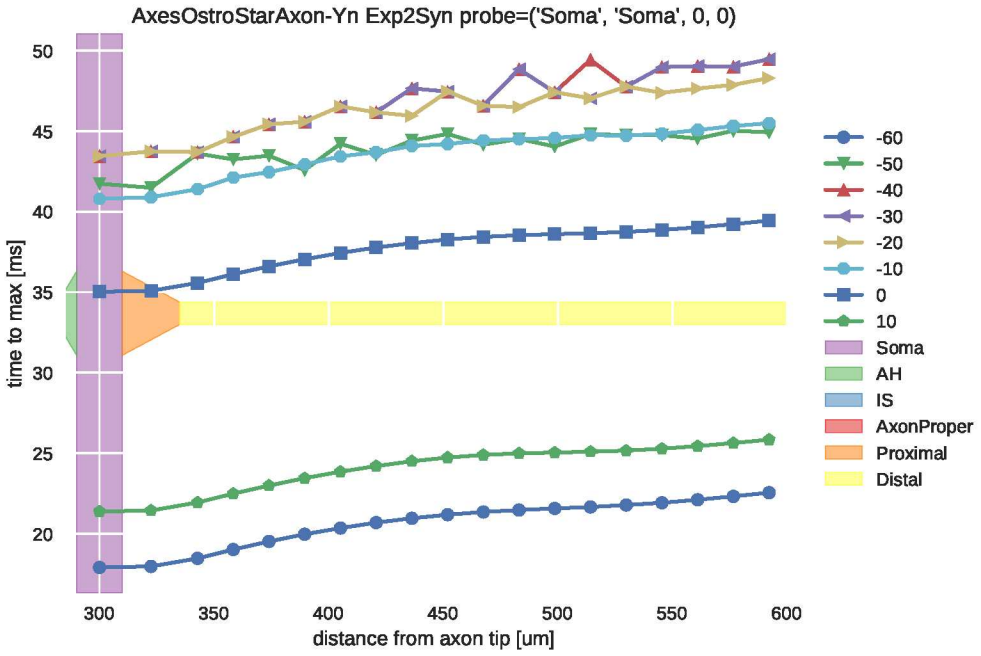

Figure 3.20: The time required for the soma to reach maximum membrane voltage (y-axis in µs) when a synapse triggered at that distance from the axon tip (x-axis) with the synapse weight necessary (see Fig. 3.19) to reach the specified membrane voltage (see legend) is triggered.

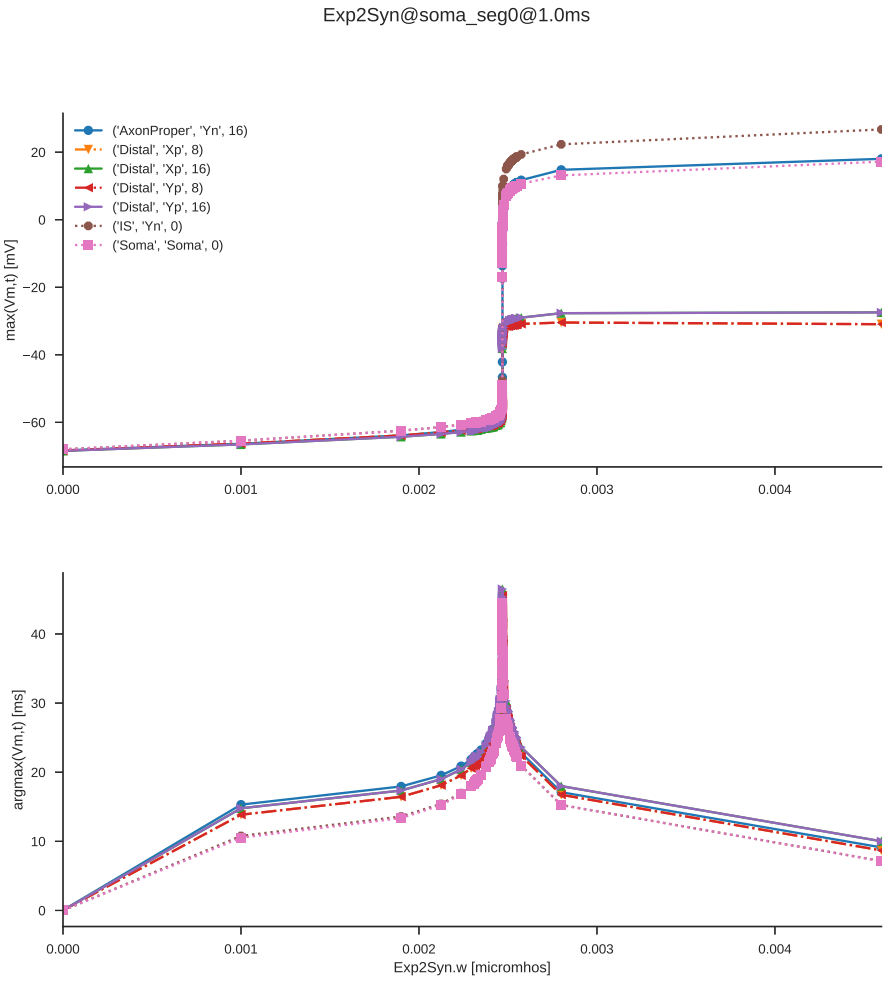

Figure 3.21: Maximum membrane voltage (top) and time to reach that maximum (from simulation start (synapse fire starts at 1ms)) (bottom) at probe locations (see legend) in the neuron when a synapse located on the soma is triggered. Top and bottom plots share the same x-axis.